water

MDPI

Article

Assessment and Modeling of the Hydrological Response of Extensive Green Roofs Under High-Intensity Simulated Rainfalls

Cristina Bondì * and Massimo Iovino

Department of Agricultural, Food and Forest Sciences, University of Palermo, 90128 Palermo, Italy; massimo.iovino@unipa.it

* Correspondence: cristina.bondi@unipa.it

Abstract

Rainfall retention and runoff detention are the key hydrological processes that reduce runoff from green roofs. This study aims to quantify and model the hydrological response of nine combinations of growing substrates and drainage layers for extensive green roofs. Retention and detention capacities were evaluated using laboratory column experiments under two extreme initial moisture conditions—air-dried (D) and field capacity (W)—and three rainfall intensities (30, 60, and 100 mm h^{-1}). Regardless of the substrate–drainage combination, retention capacity, W_R, was significantly higher under dry conditions than under wet ones. Under wet conditions and rainfall intensity of 30 mm h^{-1} (30 W tests), the mean W_R value (5.2 mm) was significantly lower than those recorded at higher intensities (14.3 and 14.2 mm, for 60 W and 100 W tests, respectively). Detention capacity, W_D, was less influenced by initial moisture and rainfall intensity, with mean values ranging from 7.4 to 10.9 mm. The distinct hydrological responses of green roof columns in the two antecedent moisture conditions were attributed to contrasting infiltration mechanisms: capillary flow dominated under dry conditions, while gravity-driven preferential flow prevailed under wet conditions. The application of a simple reservoir-routing model revealed that the AgriTerram (AT)—expanded perlite (EP) combination achieved the greatest reduction in total outflow volume and peak runoff. Under wet initial conditions, no single configuration clearly outperformed the others. This study highlights how the combined use of simulated rainfall experiments and a reservoir-routing model enables the identification of the most effective combination of substrate and drainage system to improve the hydrological performance of green roofs.

Keywords: rainfall retention; runoff detention; substrate; drainage layer; simulated rainfall; reservoir-routing model

Academic Editor: Paul Kucera

Received: 9 September 2025
Revised: 16 October 2025
Accepted: 28 October 2025
Published: 30 October 2025

Citation: Bondì, C.; Iovino, M. Assessment and Modeling of the Hydrological Response of Extensive Green Roofs Under High-Intensity Simulated Rainfalls. *Water* **2025**, *17*, 3113. https://doi.org/10.3390/w17213113

1. Introduction

Anthropogenic soil sealing—resulting from the progressive substitution of pervious surfaces with impervious materials, such as roads, parking lots, or buildings—alters the natural hydrological cycle [1]. This process inhibits water infiltration and soil absorption, resulting in a significant increase in both the peak and volume of stormwater runoff. It also shortens the lag time between peak rainfall and peak runoff compared to natural areas, thereby heightening the risk of pluvial flooding [2–4]. To counteract the negative effects of soil sealing, several natural water retention measures (NWRMs) can be adopted, including

green roofs [5,6]. A green roof, also called vegetated rooftop or eco roof, is a vegetated system made on impermeable structural supports, such as floors or roofs of buildings, which, apart from managing the quantity and quality of runoff, bring multiple benefits such as mitigation of "heat islands" [7], remediation of soil and water [8,9], reduction in noise levels [10], improvement of air quality [11], rise in biodiversity [12], thus improving the quality of life in urban and peri-urban areas. Typically, it consists of four main layers, from bottom to top: a drainage layer, a filter layer that prevents the loss of soil particles, a substrate (or growing medium) layer, and a vegetation layer [13]. The active presence of a soil–plant system facilitates, through the processes of infiltration, retention, and evapotranspiration, the capture of water and the return to the atmosphere of a significant portion of precipitation. An extensive green roof can retain, on average, between 40% and 60% of the annual amount of rainwater. However, its retention capacity may vary and be lower in response to isolated extreme precipitation events [14–16].

Green roof mitigates stormwater effects through two main hydrological processes: the rainfall retention capacity, i.e., the rainfall volume stored by the substrate that is lost through evapotranspiration, and the detention of runoff, i.e., the transient precipitation storage resulting in a delay and reduction in the peak flood output [17,18]. Both these processes are closely conditioned by the physical and hydraulic properties of the substrate–drainage system.

The substrate typically consists of mineral and organic components blended in varying proportions to maximize water retention for crop supply, while maintaining efficient drainage to prevent surface ponding and structural overload [19,20]. The drainage layer aims to drain the excess of water from the substrate, allowing a suitable equilibrium between air and water in the root zone. It can be formed from either granular materials—such as pozzolana, pumice, lapilli, expanded clay, expanded perlite, or crushed bricks—or modular plastic panels (polyethylene or polystyrene), with cavities for water storage and holes to drain the surplus water [21].

The retention capacity of the substrate is influenced by the pores size distribution, while the detention capacity depends on the hydraulic conductivity that defines the ability of the substrate to transmit water downward. However, the hydrodynamic response of a green roof also depends on several other factors, including the depth of the substrate, the vegetation cover, the slope of the roof, the rainstorm characteristics such as intensity and duration, and the presence and properties of the drainage layer [13,22,23].

Therefore, a joint characterization of the substrate–drainage system is essential for understanding its combined effect on green roof performance. Existing studies often adopt a predetermined drainage layer, without systematically evaluating its interaction with the substrate [12,24,25]. This highlights the need for an integrated approach that considers the coupled behavior of both components, as their appropriate combination is crucial for optimizing the hydrological response of the green roof and ensuring its health and durability [26,27]. Retention and detention capacity can be evaluated experimentally through simulated rain tests conducted on laboratory columns [24,28–30].

To develop applicable tools for predicting green roof hydrology across diverse climates, mechanistic and conceptual models have been applied to the simulated rain tests [23,24,31]. Physically based approaches utilizing numerical solutions of the Richards' equation have proven effective [32–34]. However, these models require an accurate physical and hydraulic characterization of the substrate, which is often hard to obtain, while green roof design demands simpler, efficient, and easily integrable models [35].

Kasmin et al. [36] proposed a conceptual rainfall-runoff model based on a reservoir-routing approach. A similar approach to extensive green roof modeling was proposed by Locatelli et al. [37]. The reservoir-routing model was applied under temperate climatic

conditions to evaluate the influence of substrate compositions and vegetation treatments on the hydrological performance of extensive green roof test beds [38–40]. It proved to yield reasonable runoff estimations and vertical moisture profiles comparable to those from a one-dimensional numerical solution of the Richards' equation [41]. Skala et al. [42] considered the reservoir-routing approach more appropriate for extensive green roofs than other hydrological models, due to its better representation of rapid responses in thin soils.

So far, limited attention has been paid to assessing how the combination of substrate and drainage layers affects the retention and detention performance of green roofs during intense rainfall events. This study aims to fill this gap by evaluating the joint influence of different substrate and drainage configurations on the retention and detention capacities of nine green roof columns exposed to simulated heavy rainfalls. The experimental design includes three rainfall intensities and two contrasting initial moisture conditions—air-dry and wet (close to field capacity)—to systematically explore how these variables shape the hydrological response of the substrate–drainage system. The goal is to identify optimal design combinations tailored to the specific needs of Mediterranean climate conditions.

2. Materials and Methods

2.1. Experimental Setup

Laboratory tests were carried out at the Department of Agriculture, Food and Forestry Sciences of the University of Palermo, Italy. The experimental setup (Figure 1) includes a rainfall simulator consisting of 45 hypodermic needles (22 Gauge, diameter of 0.7 mm) distributed over an area of 314 cm^2 connected to a loading tank that could be adjusted in height to modify the rainfall intensity. Two load cells (AZ 0-10 with full scale of 100 kg and measurement error $\leq \pm 2\%$) were used for continuous monitoring of the water content of the green roof samples and measuring the outflow volume. The signal was acquired automatically through a CR1000 datalogger (Campbell Scientific, Logan, UT, USA) at 10 s, registered with the software LoggerNet and sampled at 1 min intervals after a 9-points centered moving average smoothing.

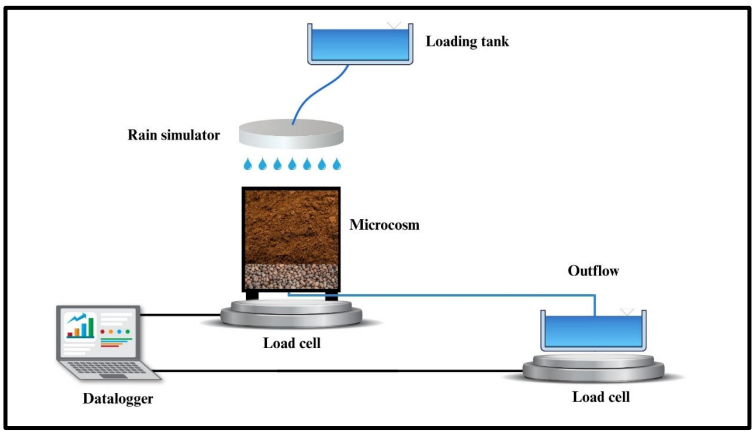

Figure 1. Scheme of the experimental setup for simulated rain tests.

The rainfall simulator was preliminarily calibrated to determine the relationship between the water head in the loading tank and the intensity of rainfall. Eight calibration tests were conducted with water heads ranging from 0 to 12 cm, which corresponded to rainfall intensities within the range from 30 to 200 mm h^{-1}, under controlled temperature conditions of approximately 20 °C. The relationship between water head and rainfall intensity was found to be linear, with a coefficient of determination, R^2, equal to 0.9986.

Green roof columns (Figure 1) were prepared into plexiglass cylinders, with an internal diameter of 19.4 cm, equipped with a central drainage hole (ϕ = 20 mm) at the bottom to

collect the outflow volume. The size of the drainage hole ensured that outflow at the base of the column was not restricted, regardless of the drainage layer used. Nine combinations of drainage layers and substrates were considered (Figure 2). Specifically, three substrates were combined with three drainage layers, each having constant thicknesses of 10.0 cm and 4.0 cm, respectively. The total height of the experimental columns was therefore less than 15.0 cm, which is commonly considered the maximum thickness for an extensive green roof. A thin geotextile (<1 cm) made of polypropylene was used to prevent fine particles from the overlying substrate from being washed into the drainage layer.

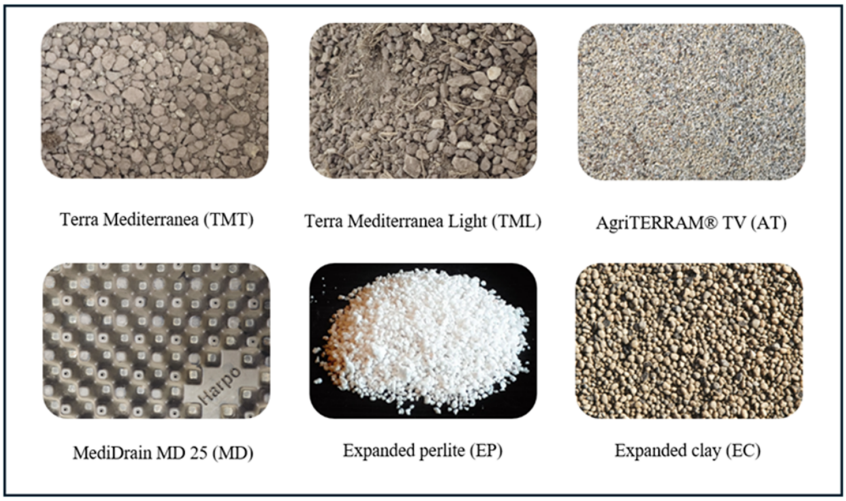

Figure 2. Growing substrates (**top**) and drainage systems (**bottom**) employed in the study.

The three drainage layers tested (Figure 2) consisted of: (i) a preformed stratified system "MediDrain MD 25" (MD) (Harpo Verdepensile, Trieste, Italy) (ii) a mineral layer composed by commercial expanded perlite (EP) (Perlite Italiana, Corsico, Milano, Italy) and (iii) an expanded clay (EC) balls layer (Leroy Merlin, Rozzano, Milano, Italy) [43]. Three commercial substrates with different characteristics were tested (Figure 2), i.e., "Terra Mediterranea" (TMT) and "Terra Mediterranea Light" (TML), both produced by Harpo Verdepensile, and "AgriTERRAM® TV" (AT), a substrate made by Perlite Italiana [44].

The water retention curves of the three substrates were determined by the Wind evaporation method [44,45] and the pressure plate apparatus [46], and the resulting data subsequently fitted using the unimodal van Genuchten model [47]. The volumetric water contents at saturation, θ_S (0 kPa), at field capacity, θ_{FC} (−10 kPa), and at the permanent wilting point, θ_{PWP} (−1500 kPa) of the three substrates are shown in Table 1, along with other relevant physical characteristics.

One-hour rainfall events with intensities i = 30, 60, and 100 mm h^{-1} were selected, corresponding, respectively, to return periods of 2, 20, and 500 years for the city of Palermo. To evaluate the hydraulic performance of the green roof under extreme climatic conditions, the first simulated rainfall event was applied to air-dried samples (D). This condition was considered representative of severe summer drought occurring in a Mediterranean climate. After 24 h, a second rainfall event was conducted to assess the hydrological response of the system under wet conditions (W). This condition corresponded to the substrate field capacity and was considered representative of the most critical scenario in terms of hydraulic behavior. To ensure consistent initial conditions for each rainfall sequence, distinct samples were used for each substrate/drainage layer combination. A total of 27 green roof columns were prepared, resulting from the combination of three substrates, three drainage layers, and three rainfall intensities. Each sample was subjected to two rainfall simulations (dry and wet initial conditions), yielding a total of 54 tests. Experiments

were not replicated, as the relatively high sample volume (≈3000 cm^3) was deemed to be representative of the real field conditions [28,29].

Table 1. Main characteristics of the materials used to prepare green roof columns (BD = bulk density; θ_S = volumetric water content at saturation; θ_{FC} = volumetric water content at field capacity; θ_{PWP} = volumetric water content at permanent wilting point; EC = electrical conductivity of 1:5 aqueous solution).

Layer	Identification	Composition	BD (g cm^{-3})	θ_S (cm^3 cm^{-3})	θ_{FC} (cm^3 cm^{-3})	θ_{PWP} (cm^3 cm^{-3})	Porosity (% V/V)	pH	EC (ds m^{-1})
Substrate	Terra Mediterranea (TMT)	Green compost, peat, lapillus, pumice and zeolite	0.939	0.475	0.289	0.073	50−60	6.0−7.8	0.05−0.25
	Terra Mediterranea Light (TML)	Lapillus, pumice, Baltic peat and green compost	0.826	0.513	0.251	0.068	60−70	7.5−8.0	0.30−0.50
	AgriTERRAM® TV (AT)	Peat, lapillus, pumice, Agrilit expanded perlite, bark, coconut fibres, special clays, organic fertilizers	0.447	0.650	0.242	0.110	>80	6.0−7.0	0.40
Drainage	MediDrain MD 25 (MD)	Preformed polystyrene	-	-	-	-	-	-	-
	Agrilit 1 expanded perlite (EP)	Expanded perlite with fine grain size	0.120	-	-	-	>90	6.5−7.5	0.02
	Expanded clay (EC)	A balls of 100% expanded clay with controlled pH	0.360	-	-	-	>80	6.5−7.0	0.80

Following De-Ville et al. [39], the retention capacity, W_R (mm), of the green roof columns was assumed equal to the depth of water, W (mm), remaining stored within the sample one hour after the end of the precipitation (t = 2 h). It is given by the difference between the total cumulative rainfall, I_{tot} (mm), and the cumulative runoff, R_{tot} (mm). The detention capacity, W_D (mm), of green roof columns was estimated as the difference between the maximum stored water W_{max}, which was reached at the end of the rainfall (t = 1 h), and W_R. This volume represents the portion of precipitation that is temporarily retained in the substrate during rainfall and released shortly afterward. Both W_R and W_D were also expressed as a percentage of total rainfall and referred to as retention performance, RP (%), and detention performance, DP (%). The runoff coefficient, RC (%), was calculated as the ratio R_{tot}/I_{tot}. The time elapsed between the onset of rainfall, and the start of runoff represents the delay in green roof response, t_d (h). It is worth noting that, at $t = t_d$, the stored rainfall is theoretically equal to W_R (Figure 3).

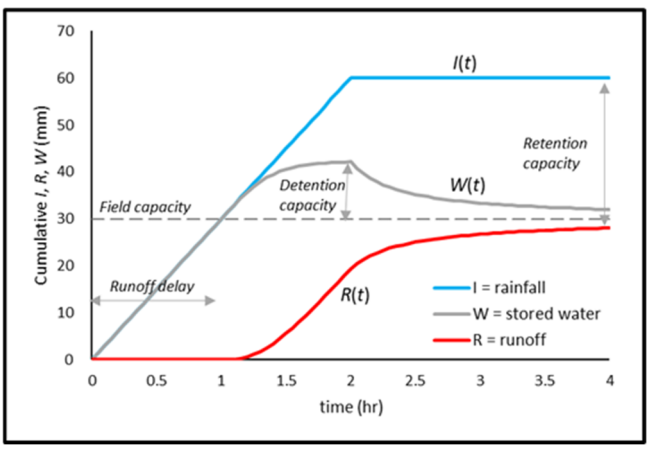

Figure 3. Schematic representation of the hydrological response of a green roof.

The reliability of the collected data was assessed by calculating the mass balance, MB (%), as the ratio between the variation in water content stored in the substrate at the end of the test [W (t = 2 h) − W (t = 0)] and the difference $I_{tot} - R_{tot}$.

2.2. Simple Reservoir-Routing Model

The simple reservoir-routing model proposed by Kasmin et al. [36] was fitted to the runoff data obtained from simulated rainfall tests. In this model rainfall is stored in the green roof up to field capacity whereas excess rainfall is temporarily retained before vertically generating runoff. At the end of the storm event, the temporary storage will drain in a relatively short time until field capacity. The storage routing equation is:

$$W_t = W_{t-1} + i\Delta t - r\Delta t \quad (1)$$

in which W (mm) represents the stored moisture depth at a given time, i and r represent, respectively, the rainfall intensity (mm h^{-1}) and the runoff flow (mm h^{-1}) out of the green roof. The latter quantity can be estimated by:

$$r = k(W_{t-1} - W_R)^n \quad (2)$$

in which k (mm$^{1\text{-n}}$) and n (-) are the reservoir-routing parameters.

Under real conditions, the value of n can be assumed as a constant, being greatly influenced by the construction characteristics of the roof, such as its slope and drainage length. This allows the model to be simplified into a single scale parameter, k, which is influenced by the substrate and vegetation [48]. However, in this study, due to the different scale dimensions of the green roof columns, both model parameters k and n were estimated by a fitting procedure, implemented into Microsoft Excel Solver, that minimizes the value of the sum of squared deviations (SSD) between the predicted and the observed runoff values. Initial losses (i.e., retention capacity) were removed from the monitored data to generate a net runoff profile before applying the reservoir-routing model. In practice, the starting point of the runoff hydrograph was translated forward in time by a duration corresponding to t_d.

2.3. Statistical Analysis

According to the Lilliefors test [49], the measured W_R and W_D data followed a normal distribution. A preliminary analysis was performed to assess the effect of initial moisture conditions. Two datasets collected under different initial moisture conditions were compared by a paired t-test, considering that the substrate–drainage layer combinations remained consistent while varying the initial moisture conditions. Subsequently, the influence of rainfall intensity on retention, W_R, and detention, W_D, capacities was evaluated. For the two datasets collected under dry (D) or wet (W) conditions, the influence of rainfall intensity on W_R and W_D was statistically checked by comparing different rainfall intensities (30 vs. 60, 30 vs. 100, and 60 vs. 100 mm h^{-1}) by a paired t-test. Finally, the role of the different substrate–drainage configurations on W_R and W_D was evaluated by a pairwise t-test, homoscedastic or heteroscedastic according to the results of a preliminary F-test. All statistical tests were conducted at a significance level of p = 0.05.

The considered conceptual model was evaluated by comparing simulated and measured runoff values [23]. For this purpose, according to Zhang et al. [22], the Nash-Sutcliffe

Efficiency (*NSE*) [50], the coefficient of determination (R^2), and the percentage bias (*PBIAS*) were calculated for each simulated rainfall test.

$$NSE = 1 - \frac{\sum_{i=1}^{n}\left(r_i^{obs} - r_i^{sim}\right)^2}{\sum_{i=1}^{n}\left(r_i^{obs} - \bar{r}^{obs}\right)^2} \quad (3)$$

$$R^2 = \left\{ \frac{\sum_{i=1}^{n}\left(r_i^{obs} - \bar{r}^{obs}\right)\left(r_i^{sim} - \bar{r}^{sim}\right)}{\left[\sum_{i=1}^{n}\left(r_i^{obs} - \bar{r}^{obs}\right)^2 \sum_{i=1}^{n}\left(r_i^{sim} - \bar{r}^{sim}\right)^2\right]^{0.5}} \right\}^2 \quad (4)$$

$$PBIAS = \frac{\sum_{i=1}^{n} r_i^{sim} - \sum_{i=1}^{n} r_i^{obs}}{\sum_{i=1}^{n} r_i^{obs}} \times 100 \quad (5)$$

in which r_i^{obs} and r_i^{sim} are the observed and the simulated runoff rates at time i, respectively; $\bar{r}^{obs}$ and $\bar{r}^{sim}$ are the mean values of the observed and simulated data, respectively.

3. Results and Discussion

3.1. Hydrological Performance of Green Roof Columns

The green roof columns exhibited a hydrological response that was strongly dependent on both the initial moisture conditions and the simulated rainfall intensity (Table 2). Regardless of the substrate–drainage combination, no runoff was observed for initial dry conditions with a rainfall intensity of 30 mm h^{-1} (30 D). The green roof columns retained the entire one-hour rainfall volume (i.e., $W_R \geq 30$ mm), indicating a delay in runoff formation exceeding 1 h. Detention capacity could not be determined, and the runoff coefficient was zero. In more than half of the experiments considered (N = 45), the mass balance did not exceed the generally accepted threshold of 90%. The observed discrepancies were attributed to unforeseeable factors, such as variations in water temperature and sporadic clogging of simulator needles during operation, that affected the actual rainfall intensity, particularly under low-intensity conditions (Table 2).

For the experiments conducted under initial dry conditions at rainfall intensities of 60 mm h^{-1} (60 D) and 100 mm h^{-1} (100 D), the retention capacity was generally greater than 30 mm and, on average, equal to 37.6 and 35.8 mm for 60 D and 100 D, respectively. It is noteworthy that the W_R values exceeded the substrate's field capacity—ranging from 24 to 29 mm (Table 1)—as a result of the additional water retention provided by the drainage layer. For both rainfall intensities, the maximum value of W_R was observed for the TMT-EP combination and the minimum value for TML-MD one (Table 2). As expected, the runoff formation was 0.56 times more rapid for 100 D compared to 60 D. In agreement with W_R values, t_d was maximum for TMT-EP and minimum for TML-MD. The detention capacity, W_D, was lower and approximately two times more variable than W_R (Table 2).

The retention and detention performances and the runoff coefficients were affected by the total cumulative inflow volume. Increasing the total cumulative rainfall from 60 to 100 mm, i.e., by a factor of 1.67, determined an average decrease in mean RP and DP by a factor of 1.75 and 1.77, respectively, and an increase in mean RC by a factor of 1.65.

Under initially wet conditions (W), the mean retention capacity was considerably lower and more variable than under dry (D) conditions (Table 2). The delay t_d did not follow a clear trend with mean value at intermediate rainfall intensity (60 W) that was greater than either at lower (30 W) and higher (100 W) intensities. Detention capacity showed mean values comparable with those obtained under dry conditions, albeit with greater variability, ranging from a mean of 7.4 mm at rainfall intensities of 30 and 60 mm h^{-1} to 10.9 mm at 100 mm h^{-1}. In contrast to dry tests, a clear prevalence of a given substrate–drainage layer configuration over the others was not detectable. For instance, the TMT-EP combination,

which achieved the highest W_R in the D tests regardless of the applied rainfall intensity, showed its best performance only at 30 W (W_R = 8.5 mm). The specific response of the tests conducted on initially wet green roof columns was further confirmed by the trend of performance parameters (i.e., RP, DP, and RC). Only the detention performance decreased at increasing *i*, as expected, even if not at a proportional rate. At the highest rainfall intensity, an increase in the inflow volume by a factor of 1.67 only determined a decrease in DP by a factor of 1.13. The other two performance parameters showed the maximum (RP = 23.7%) and the minimum values (RC = 77%) at the intermediate rainfall intensity.

Table 2. Hydrological response of green roof columns in initial dry (D) and wet (W) conditions, at rainfall intensities of 30, 60, and 100 mm h^{-1} (t_d = runoff delay; W_R = retention capacity; W_D = detention capacity; RP = retention performance; DP = detention performance; RC = runoff coefficient; MB = mass balance).

ID	t_d (h)	W_R (mm)	W_D (mm)	RP (%)	DP (%)	RC (%)	MB (%)	t_d (h)	W_R (mm)	W_D (mm)	RP (%)	DP (%)	RC (%)	MB (%)
				30D							30W			
TMT-MD	≥1.00	≥30.0	n.d.	100.0	n.d.	0.00	n.d.	0.20	6.5	9.9	21.7	32.9	87.8	73.6
TMT-EP	≥1.00	≥30.0	n.d.	100.0	n.d.	0.00	n.d.	0.18	8.5	9.1	28.3	30.4	90.5	79.5
TMT-EC	≥1.00	≥30.0	n.d.	100.0	n.d.	0.00	n.d.	0.13	6.9	10.9	23.1	36.2	94.7	77.6
TML-MD	≥1.00	≥30.0	n.d.	100.0	n.d.	0.00	n.d.	0.15	6.5	7.7	21.7	25.8	89.9	80.4
TML-EP	≥1.00	≥30.0	n.d.	100.0	n.d.	0.00	n.d.	0.02	1.0	6.7	3.5	22.4	84.7	81.1
TML-EC	≥1.00	≥30.0	n.d.	100.0	n.d.	0.00	n.d.	0.05	1.9	5.3	6.3	17.6	84.6	83.5
AT-MD	≥1.00	≥30.0	n.d.	100.0	n.d.	0.00	n.d.	0.15	6.5	3.5	21.8	11.7	85.5	89.0
AT-EP	≥1.00	≥30.0	n.d.	100.0	n.d.	0.00	n.d.	0.03	1.5	4.7	5.0	15.7	65.4	86.1
AT-EC	≥1.00	≥30.0	n.d.	100.0	n.d.	0.00	n.d.	0.27	7.5	8.6	25.0	28.7	84.0	76.7
mean								*0.13*	*5.2*	*7.4*	*17.4*	*24.6*	*85.2*	*80.8*
CV (%)								*63.5*	*55.2*	*33.9*	*55.2*	*33.9*	*9.7*	*5.9*
				60D							60W			
TMT-MD	0.58	35.1	7.1	58.5	11.9	35.6	88.4	0.10	6.7	3.2	11.2	5.3	86.8	94.1
TMT-EP	0.78	52.4	8.5	87.3	14.2	19.5	88.5	0.10	7.3	4.9	12.1	8.2	87.5	92.2
TMT-EC	0.52	37.7	6.6	62.9	11.0	45.5	91.3	0.10	7.7	2.2	12.8	3.6	87.2	96.5
TML-MD	0.42	26.7	14.3	44.4	23.9	53.6	80.1	0.15	13.6	16.1	22.6	26.9	79.5	80.4
TML-EP	0.47	35.8	7.3	59.6	12.2	47.3	90.3	0.22	14.8	7.3	24.7	12.1	75.2	89.2
TML-EC	0.60	36.6	8.5	61.0	14.2	37.5	87.3	0.15	14.0	6.5	23.3	10.9	79.2	91.1
AT-MD	0.58	34.8	15.3	58.0	25.5	39.7	79.0	0.30	23.3	14.0	38.8	23.3	64.8	82.6
AT-EP	0.77	46.8	5.4	78.0	9.0	18.4	91.4	0.35	28.4	8.5	47.4	14.2	57.3	88.6
AT-EC	0.42	32.2	1.0	53.7	1.6	52.3	98.6	0.17	12.1	4.0	20.2	6.7	80.0	93.7
mean	*0.57*	*37.6*	*8.2*	*62.6*	*13.7*	*38.8*	*88.3*	*0.18*	*14.2*	*7.4*	*23.7*	*12.4*	*77.5*	*89.8*
CV (%)	*23.7*	*20.4*	*53.1*	*20.4*	*53.1*	*33.1*	*6.7*	*50.0*	*52.0*	*64.7*	*52.0*	*64.7*	*13.4*	*6.0*
				100D							100W			
TMT-MD	0.32	36.5	14.5	36.5	14.5	65.7	88.0	0.08	10.6	1.5	10.6	1.5	87.8	98.3
TMT-EP	0.47	51.1	5.0	51.1	5.0	45.6	94.9	0.08	9.3	9.4	9.3	9.4	90.5	91.2
TMT-EC	0.33	40.6	5.3	40.6	5.3	62.5	95.3	0.03	6.4	5.5	6.4	5.5	94.7	95.6
TML-MD	0.18	20.9	12.2	20.9	12.2	80.7	89.8	0.08	9.2	23.8	9.2	23.8	89.9	79.3
TML-EP	0.37	39.4	9.6	39.4	9.6	54.8	90.0	0.12	14.0	11.1	14.0	11.1	84.7	89.2
TML-EC	0.20	23.6	9.5	23.6	9.5	78.3	92.0	0.13	16.1	15.5	16.1	15.5	84.6	87.2
AT-MD	0.33	38.4	3.2	38.4	3.2	62.5	97.0	0.12	14.8	10.4	14.8	10.4	85.5	90.8
AT-EP	0.42	42.5	5.6	42.5	5.6	57.0	94.6	0.30	31.6	9.9	31.6	9.9	65.4	90.2
AT-EC	0.27	29.5	4.4	29.5	4.4	69.9	95.7	0.13	16.9	11.4	16.9	11.4	84.0	90.2
mean	*0.32*	*35.8*	*7.7*	*35.8*	*7.7*	*64.1*	*93.0*	*0.12*	*14.3*	*10.9*	*14.3*	*10.9*	*85.2*	*90.2*
CV (%)	*29.1*	*26.8*	*50.7*	*26.8*	*50.7*	*17.4*	*3.4*	*61.9*	*51.6*	*56.8*	*51.6*	*56.8*	*9.7*	*5.9*

The different hydrological responses of green roof columns under dry and wet conditions can be attributed to the different mechanisms that govern infiltration in substrates. Under dry conditions, water infiltration is mainly driven by capillarity that yields a more uniform wetting of the porous medium. The retention capacity is not affected by the rainfall intensity, and it approaches the maximum value (on average 35 mm, considering the contribution of the drainage layer). Variability in W_R is similar for the two tested intensities and primarily depends on the substrate–drainage layer combination. Thanks to a more uniform wetting of the sample, the runoff coefficient, as well as other green roof performance parameters (RP and DP), was closely linked to the total inflow volume.

Under wet conditions, a large portion of the substrate total porosity is nearly saturated, which limits further water absorption [17]. Water primarily moves through the largest interconnected pores, making infiltration primarily driven by gravity [51]. With reduced available porosity, the retention capacity becomes lower and more variable, while rapid preferential flows can trigger sudden runoff at the bottom of the sample. As a result, the delay times are erratic and not closely correlated with rainfall intensity. The green roof detention capacity—occurring when the substrate is at its field capacity—is mainly governed by fast gravity-driven flows and was therefore similar under both initial conditions (D or W). The observed differences were likely more influenced by the specific combination of substrate and drainage layer.

3.2. Statistical Evaluation of the Hydrological Performance of Green Roof Columns

Since no runoff was observed in the 30 D tests, the influence of initial conditions on green roof retention and detention capacities was tested only for i = 60 and 100 mm h^{-1}.

Paired t-tests showed that mean retention capacity, W_R, was significantly higher under dry conditions, while mean detention, W_D, showed no significant difference. These findings confirm that the initial green roof moisture condition affects retention but not detention, aligning with previous studies. For instance, Czemiel Berndtsson [13] demonstrated that antecedent moisture conditions exert a pivotal influence in determining the amount of water retained and the portion of runoff reduced. Similarly, Liu et al., [52] reported a statistically significant positive correlation between initial substrate moisture content and the runoff coefficient, indicating that wetter initial conditions tend to result in higher runoff generation. In alignment with these observations, Villarreal & Bengtsson [53] found that substrates that are dry before a rainfall event exhibit significantly greater stormwater retention capacity compared to those that are already wet.

Given initial moisture conditions influenced W_R but not W_D, the influence of rainfall intensity on W_R was separately analyzed for the D and W datasets. This resulted in two statistical comparisons for dry conditions (i.e., 60 D vs. 100 D) and three statistical comparisons for wet conditions (i.e., 30 W vs. 60 W, 30 W vs. 100 W and 60 W vs. 100 W). For the detention capacity, the results obtained for D and W tests at a given rainfall intensity were pooled together, and three pairwise t-tests were conducted (Table 3).

Table 3. p-values of pairwise t-tests aimed at investigating the effects of rainfall intensity on the green roof retention, W_R, and detention, W_D, capacities.

	W_R		W_D
	D	**W**	**D + W**
30–60	-	0.019	0.786
30–100	-	0.019	0.745
60–100	0.366	0.940	0.364

Retention capacity under initial dry conditions was independent of the rainfall intensity. In contrast, for initial wet conditions, the tests conducted at 60 and 100 mm h^{-1} yielded significantly higher W_R values than those at 30 mm h^{-1}. Substrates that are far from saturation—effectively empty—can retain a large fraction of rainfall due to capillarity, independently of intensity. Breulmann et al. [54] showed that a dry substrate can retain up to 99% of precipitation, confirming the importance of the initial moisture condition. Near saturation, total retention capacity decreases, and rainfall intensity may influence performance. Under wet conditions, water flow is primarily driven by fast gravity flow. At low rainfall intensity, preferential flow paths tend to concentrate in a smaller portion of the sample volume, reducing the likelihood of matrix adsorption. As rainfall intensity increases, a larger volume of substrate is affected by preferential flow, allowing more matrix

pores to retain rainfall. Our results also suggest that beyond a certain threshold of rainfall intensity (i.e., 60 mm h^{-1}), further increases in the substrate's retention capacity should not be expected. This aligns with literature showing retention increases at low–moderate intensities but declines at higher ones, resembling runoff from gray roofs [55–58].

The rainfall intensity did not influence the detention capacity of the green roof columns (Table 3). This confirms that the temporary storage of water in the green roof column, once the field capacity is reached, mainly depends on the saturated (or near-saturated) hydraulic conductivity of the substrate and the physical characteristics of the drainage layer [44].

3.3. Influence of Substrate–Drainage Combination on the Hydrological Response

Building on the previous analyses, the effect of substrate type and the drainage layer on W_R and W_D was evaluated by grouping data across the other factors (i.e., drainage or substrate), which were treated as replicates. According to the results discussed in the previous section, three groups were considered for W_R: (i) initial dry conditions (N = 6); (ii) initial wet conditions and low rainfall intensity (N = 3); (iii) initial wet conditions and high rainfall intensity (N = 6). Only a single group was considered for W_D (N = 15).

Under dry conditions, the best retention (W_R = 42.2 mm) was observed for TMT, followed by AT (W_R = 37.4 mm) and TML (W_R = 30.5 mm) according to a significant order TMT ≥ AT ≥ TML (Figure 4a). Under wet conditions, different findings were obtained according to the applied rainfall intensity. At the lowest rainfall intensity, mean W_R values ranged between 3.1 and 7.1 mm (TMT = AT = TML) (Figure 4b), whereas, at higher rainfall intensity, TML and AT performed significantly better than TMT (AT = TML > TMT) (Figure 4c). Detention capacity was significantly higher for TML (W_D = 10.8 mm), whereas TMT and AT showed similar mean WD values (6.9 and 7.3 mm, respectively) (Figure 4d).

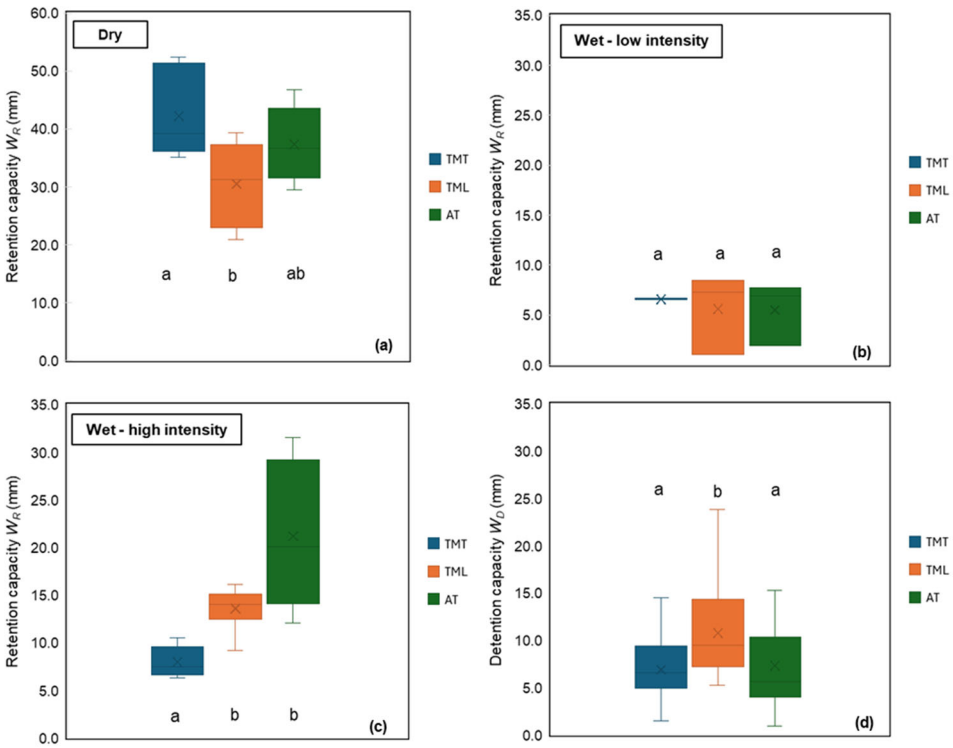

Figure 4. Hydrological response of the three substrates (TMT = Terra Mediterranea, TML = Terra Mediterranea Light, AT = AgriTERRAM® TV): (**a**) retention capacity under initial dry conditions; (**b**) retention capacity under initial wet conditions and i = 30 mm h^{-1}; (**c**) retention capacity under initial wet conditions and $i \geq 60$ mm h^{-1}; (**d**) detention capacity. Mean values with the same letter did not differ significantly according to a pairwise t-test ($p < 0.05$).

The AT substrate showed a good retention capacity to store and save water for crop requirements, which is supported by its high porosity (>80%) as reported in Table 1. On the other hand, the relatively large pores that characterize this substrate can promote rapid drainage once the field capacity is reached [59]. Consequently, the temporary water storage is limited, as confirmed by the relatively low W_D values (Figure 4d).

The TMT substrate showed good retention capacity in initial dry conditions, but its performance declined under wet conditions, probably because of the lowest porosity. Among the three considered substrates, TML showed the highest detention capacity and acceptable retention capacity under wet conditions that are the most severe in terms of green roof hydrological response. Such behavior can be explained by a dual porosity network with micro-pores that retain water even when the substrate is already wet and macro-pores that facilitate infiltration and drainage when dry, while also prolonging water detention when the substrate is moist [60,61].

Unlike substrates, the drainage layers (MD, EP and EC) influenced green roof hydrological performance only under dry conditions. The combination including EP drainage layer showed the highest water retention capacity (W_R = 44.7 mm) followed by EC and MD (W_R = 33.4 and 32.0 mm, respectively) (Figure 5a). No statistically significant differences were found for the other comparisons, suggesting that the choice of the drainage layer is less influential than substrate selection (Figure 5b–d).

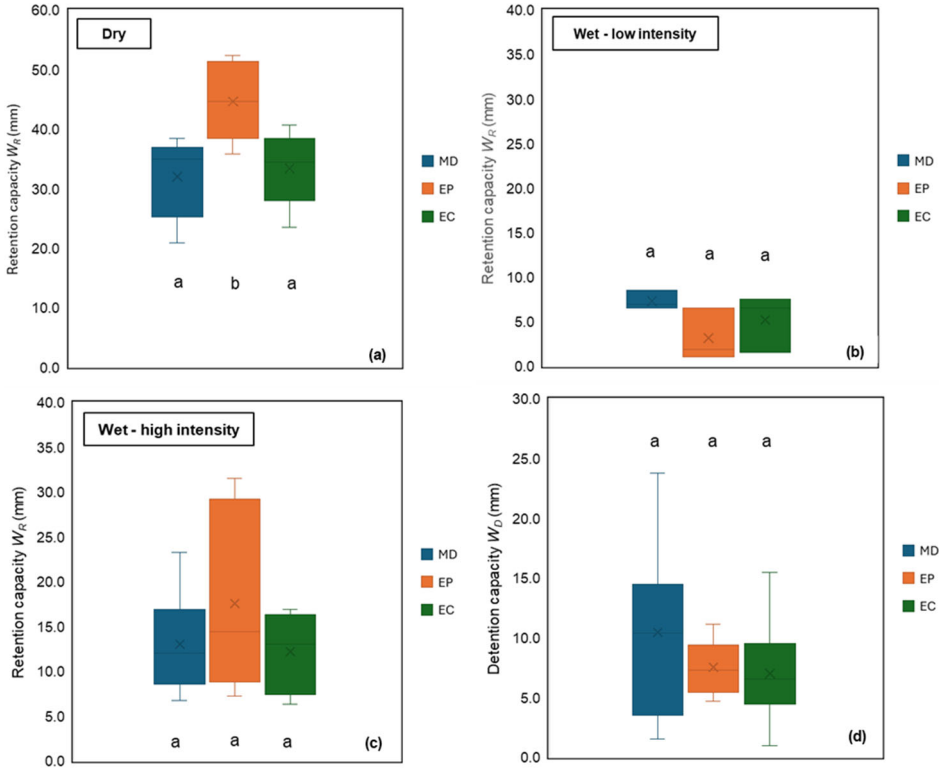

Figure 5. Hydrological response of the three drainage layers (MD = MediDrain MD 25, EP = expanded perlite, EC = expanded clay): (**a**) retention capacity under initial dry conditions; (**b**) retention capacity under initial wet conditions and i = 30 mm h^{-1}; (**c**) retention capacity under initial wet conditions and $i \geq 60$ mm h^{-1}; (**d**) detention capacity. Mean values with the same letter did not differ significantly according to a pairwise t-test ($p < 0.05$).

Expanded perlite's higher retention capacity under dry conditions can be attributed to its granular and porous structure (Figure 2), which promotes the formation of capillary bridges within intergranular voids. In contrast, expanded clay's smoother, spherical particles (Figure 2) limit capillary connectivity, reducing water retention. Pęczkowski et al. [62]

reported similar results, with perlite achieving up to 65% peak runoff reduction versus 49% for expanded clay. Compared to perlite, the preformed plastic MD layer exhibited worse WR characteristics under dry conditions but had a relatively higher detention capacity (Figure 5d). For this drainage layer, the presence of cups (Figure 2) allowed higher, although not statistically significant, water storage during rainfall, with runoff occurring only when these reservoirs are full. However, the high standard deviation associated with W_D of the MD system raises concerns about the consistency of this mechanism. Indeed, likely due to preferential flow occurring in the overlying substrate or irregular contact with the geotextile filter, uneven filling of the MD cups was observed when the samples were disassembled at the end of the experiments.

It is worth noting that an effective drainage system must prevent the occurrence of ponding phenomena. In this study, no such condition was observed under any rainfall intensity for the tested substrate–drainage layer combinations.

3.4. Simple Reservoir-Routing Model Evaluation

Runoff hydrographs are presented in Figures 6 and 7, for experiments conducted under dry and wet initial conditions, respectively. For clarity, only the modeled hydrographs are shown as the measured and simulated data exhibited near-perfect agreement as confirmed by the high values of Nash–Sutcliffe Efficiency (mean NSE = 0.97), coefficient of determination (mean R^2 = 0.99), and low values of Percent Bias (mean PBIAS = −0.149). The slightly negative value of PBIAS indicates that the model yielded a minimal overestimation of measured runoff. For 60 D experiments, the runoff hydrograph for AT-EC combination could not be determined, as the fitting technique resulted in a physically meaningless value of $n = 0$.

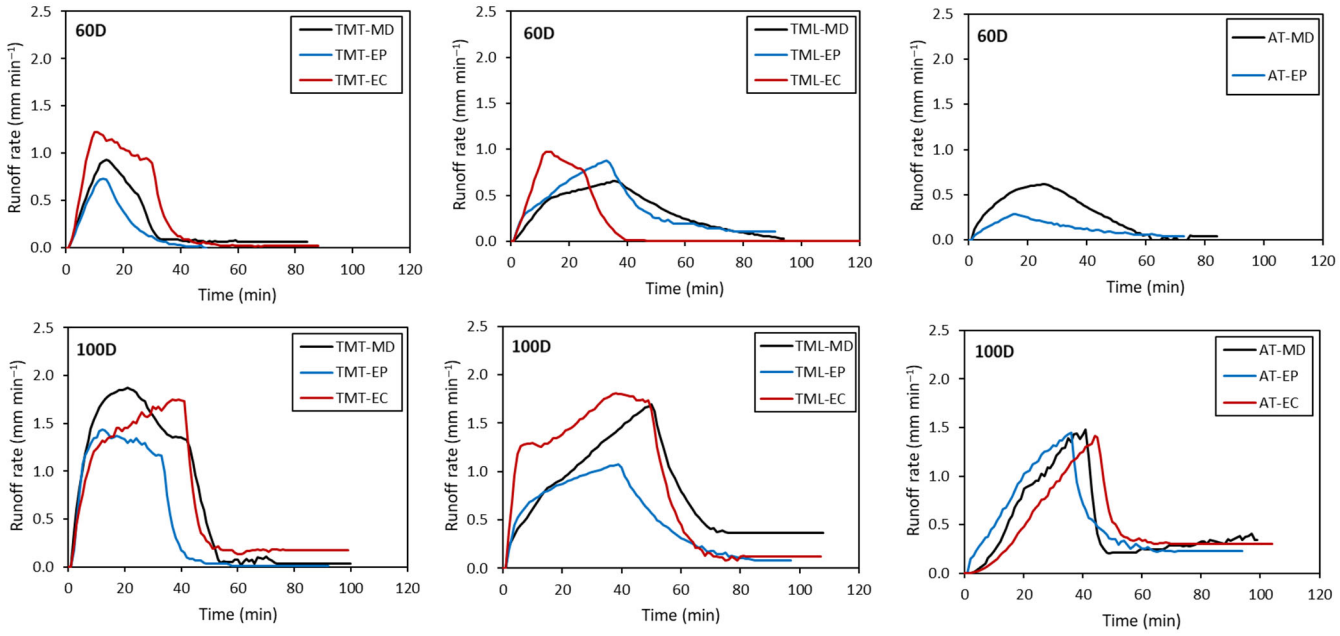

Figure 6. Runoff hydrographs for green roof columns under initial dry moisture conditions for rainfall intensities of 60, and 100 mm h^{-1} (TMT = Terra Mediterranea, TML = Terra Mediterranea Light, AT = AgriTERRAM® TV, MD = MediDrain MD 25, EP = expanded perlite, EC = expanded clay).

It is worth nothing that the hydrograph peaks were not synchronous, and the maximum runoff rates were not the same as a consequence of the different retention capacity of the green roof columns. However, excluding the influence of retention characteristics, it facilitated a more direct comparison of the dynamic detention behavior of the substrate–drainage layer system under different initial conditions and rainfall intensities.

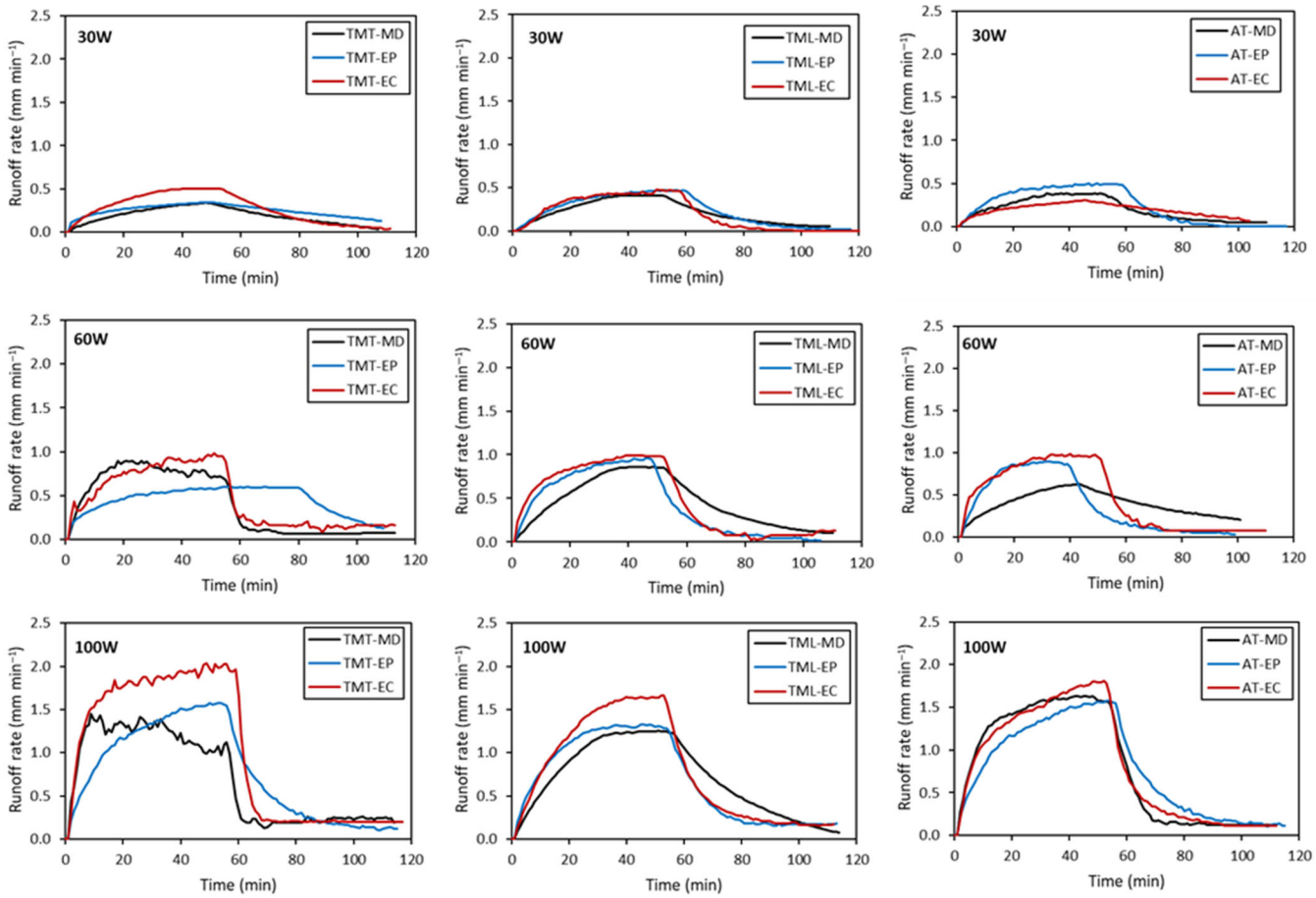

Figure 7. Runoff hydrographs for green roof columns under initial wet moisture conditions for rainfall intensities of 30, 60, and 100 mm h^{-1} (TMT = Terra Mediterranea, TML = Terra Mediterranea Light, AT = AgriTERRAM® TV, MD = MediDrain MD 25, EP = expanded perlite, EC = expanded clay).

As a general remark, the results clearly indicate that the runoff rate (mm min^{-1}) increases as rainfall intensity rises, in agreement with findings reported by Czemiel Berndtsson [13] and Wu et al., [63]. Furthermore, under constant rainfall intensity, the runoff response is influenced by the initial moisture content of the substrate, as also reported by Ferrans et al. [64]. Specifically, experiments conducted under initial wet moisture conditions yielded higher total runoff volumes and a more prolonged runoff duration than the corresponding experiments that started from dry conditions.

Regardless of substrate type, green roof columns equipped with the EC drainage system consistently exhibited the poorest performance in terms of runoff rate. Indeed, runoff rate rose suddenly and reached higher peak rate. In some cases, specifically the 60 D tests with TMT, the 100 D tests with TML, and the 100 W tests with TMT, the runoff rate temporarily exceeded the applied rainfall intensity of 1.00 and 1.67 mm min^{-1}, respectively. This can be ascribed to the delayed release of water retained within the system as the substrate approaches saturation. Expanded clay cannot absorb it in the intragranular micropores and, therefore, it is rapidly discharged through the intergranular macropores in combination with the ongoing rainfall, generating a transient peak in runoff that momentarily overcomes the rainfall input. These findings indicate that, under the tested conditions, the EC drainage system is hydrologically less efficient than the other drainage systems. Such limitations reduce retention capacity and outflow delay, ultimately increasing both runoff peak and volume. Green roof columns equipped with the EP drainage system exhibited the best performance under dry initial conditions, with lower runoff rates and improved hydraulic

response. For the wet experiments, differences between the EP and MD drainage systems were less pronounced, and the hydrological efficiency can be considered comparable.

Regarding the combined behavior of the substrate and drainage layer, the AT–EP configuration produced the highest reduction in peak runoff and the smallest total runoff volume. Under wet conditions, the differences among substrate–drainage layer combinations were nuanced, making it difficult to identify a clearly superior configuration, particularly at low rainfall intensity (Figure 7). Nonetheless, a general trend emerged, with TML and AT, combined with either EP or MD, outperforming the TMT combination.

No trend was detected in the behavior of the *k* parameter concerning initial moisture conditions and rainfall intensity (Table 4), thus confirming that this parameter is independent of external conditions as reported by Yio et al. [24], who noted a limited sensitivity of *k* to variations in rainfall intensity. In contrast, the parameter *n* tended to increase, on average, with increasing rainfall intensity under both dry and wet conditions, suggesting a potential sensitivity of this parameter to rainfall dynamics. For a typical extensive green roof, Stovin et al., [65] reported values of $k = 0.03$ mm$^{(1-n)}$ min^{-1} and $n = 2.0$, derived from plot-scale test beds. These values are broadly consistent with those obtained in this study, although slight discrepancies can be ascribed to the different spatial scales at which the processes were investigated.

Table 4. Reservoir routing parameters *k* (mm$^{1\text{-}n}$ min^{-1}) and *n* (-) and sum of squared deviations SSD between measured and simulated runoff rate for the experiments conducted under dry (D) and wet (W) conditions, at rainfall intensities of 30, 60, and 100 mm h^{-1}.

ID	k	n	SSD	k	n	SSD	k	n	SSD
		30D			60D			100D	
TMT-MD	-	-	-	0.10	1.07	4.535	0.27	0.72	8.112
TMT-EP	-	-	-	0.07	1.07	1.878	0.08	1.64	0.609
TMT-EC	-	-	-	0.08	1.45	2.175	0.09	1.54	9.286
TML-MD	-	-	-	0.04	1.01	0.939	0.13	0.93	27.887
TML-EP	-	-	-	0.12	0.95	4.189	0.12	0.93	6.006
TML-EC	-	-	-	0.12	0.99	3.643	0.25	0.87	9.479
AT-MD	-	-	-	0.13	0.56	2.884	0.01	2.07	38.445
AT-EP	-	-	-	0.07	1.07	1.878	0.08	1.64	0.609
AT-EC	-	-	-	-	-	-	0.01	1.90	40.644
Mean	-	-	-	0.09	1.02	2.765	0.12	1.36	15.675
σ	-	-	-	0.03	0.24	1.265	0.09	0.50	15.712
		30W			60W			100W	
TMT-MD	0.06	0.72	0.388	0.13	1.34	1.588	0.11	2.16	28.937
TMT-EP	0.11	0.47	1.006	0.22	0.62	2.037	0.12	1.09	13.839
TMT-EC	0.08	0.78	0.316	0.24	1.29	12.993	0.10	1.54	12.259
TML-MD	0.04	1.03	0.218	0.04	1.04	0.960	0.05	1.00	1.942
TML-EP	0.05	1.10	0.268	0.10	1.10	1.176	0.11	0.97	7.354
TML-EC	0.04	1.47	0.655	0.20	0.79	2.160	0.07	1.11	5.951
AT-MD	0.08	1.10	0.816	0.09	0.67	3.406	0.15	0.99	4.019
AT-EP	0.11	0.47	1.006	0.22	0.62	2.037	0.12	1.09	13.839
AT-EC	0.09	0.53	0.870	0.19	1.04	3.178	0.10	1.13	5.648
Mean	0.07	0.85	0.616	0.16	0.94	3.282	0.10	1.23	10.421
σ	0.03	0.34	0.322	0.07	0.28	3.731	0.03	0.39	8.175

4. Conclusions

Green roof's retention and detention capacity can be improved with an optimal choice of substrate–drainage systems. However, most of the existing studies focus on growing substrate characterization without considering its interaction with the drainage layer. This

study was conducted with the aim to fill this gap and retrieve practical indications for green roof design.

Results showed that the initial moisture conditions influenced retention capacity but not detention capacity. Under wet initial conditions, the retention capacity increased with higher rainfall intensity. In contrast, retention capacity under dry conditions and detention capacity—regardless of the initial moisture state—were not affected by rainfall intensity. The distinct hydrological responses of green roof columns were attributed to different infiltration mechanisms under the two antecedent moisture conditions. In dry conditions, capillarity leads to uniform wetting and stable retention capacity, independent of rainfall intensity. In wet conditions, partially saturated porosity limits absorption and retention capacity is affected by occurrence of gravity-driven preferential flows. Detention capacity remains similar across conditions, with differences mainly influenced by the substrate–drainage layer combination.

Among the nine combinations of growing media and drainage layers, the AT-EP one performed best -especially at higher rainfall intensities (i = 60 and 100 mm h^{-1})- achieving W_R values between 28.4 and 31.6 mm, comparable to those observed under dry conditions. Regarding detention, TML and AT combined with either EP or MD likely yielded the best results. The superior performance of the AT-EP combination was confirmed by the results of the reservoir-routing model that highlighted the greatest reduction in total outflow volume and peak runoff.

Although this investigation was conducted on a relatively small scale, its novelty lies in the comprehensive assessment of substrate–drainage combinations, achieved through the combined use of simulated rainfall experiments and a simple reservoir-routing model. This approach enabled the identification of the most effective configurations of growing media and drainage layers. Future research will focus on testing the reliability of the model's estimated parameters at larger spatial scales and evaluating the influence of vegetation on retention capacity, runoff delay, and peak flow attenuation, which is expected to affect both surface and subsurface dynamics through interception, root development, and evapotranspiration.

Author Contributions: Conceptualization, M.I.; methodology, C.B. and M.I.; formal analysis, C.B. and M.I.; investigation, C.B.; data curation, C.B. and M.I.; writing—original draft preparation, C.B. and M.I.; writing—review and editing, C.B. and M.I. All authors have read and agreed to the published version of the manuscript.

Funding: This study was funded by Ministero dell'Università e della Ricerca of Italy, project PRIN 2022 PNRR "Nature Based Solutions to enhance storage and quality of stormwater in Mediterranean peri-urban areas (NBS4STORWATER)" Next Generation EU, M4C2, CUP B53D23023760001, Codice Progetto: P2022YRXJZ.

Data Availability Statement: The original contributions presented in this study are included in the article. Further inquiries can be directed to the corresponding author.

Conflicts of Interest: The authors declare no conflicts of interest.

References

1. Scalenghe, R.; Ajmone Marsan, F. The anthropogenic sealing of soils in urban areas. *Landsc. Urban Plan.* **2009**, *90*, 1–10. [CrossRef]
2. Tobias, S.; Conen, F.; Duss, A.; Wenzel, L.M.; Buser, C.; Alewell, C. Soil sealing and unsealing: State of the art and examples. *Land Degrad. Dev.* **2018**, *29*, 2015–2024. [CrossRef]
3. Bengtsson, L. Peak flows from thin sedum-moss roof. *Hydrol. Res.* **2005**, *36*, 269–280. [CrossRef]
4. Güneralp, B.; Güneralp, I.; Liu, Y. Changing global patterns of urban exposure to flood and drought hazards. *Glob. Environ. Change* **2015**, *31*, 217–225. [CrossRef]

5. Lee, J.Y.; Lee, M.J.; Han, M. A pilot study to evaluate runoff quantity from green roofs. *J. Environ. Manag.* **2015**, *152*, 171–176. [CrossRef]
6. Shafique, M.; Kim, R.; Kyung-Ho, K. Green roof for stormwater management in a highly urbanized area: The case of Seoul, Korea. *Sustainability* **2018**, *10*, 584. [CrossRef]
7. Santamouris, A. Cooling the cities—A review of reflective and green roof mitigation technologies to fight heat island and improve comfort in urban environments. *Sol. Energy* **2014**, *103*, 682–703. [CrossRef]
8. Rowe, B. Green roofs as a means of pollution abatement. *Environ. Pollut.* **2011**, *159*, 2100–2110. [CrossRef]
9. Li, Y.; Babcock Jr, R.W. Green roofs against pollution and climate change. A review. *Agron. Sustain. Dev.* **2014**, *34*, 695–705. [CrossRef]
10. Van Renterghem, T. Green roofs for acoustic insulation and noise reduction. In *Nature Based Strategies for Urban and Building Sustainability*; Butterworth-Heinemann: Oxford, UK, 2018; pp. 167–179.
11. Yang, J.; Yu, Q.; Gong, P. Quantifying air pollution removal by green roofs in Chicago. *Atmos. Environ.* **2008**, *42*, 7266–7273. [CrossRef]
12. Wang, L.; Wang, H.; Wang, Y.; Che, Y.; Ge, Z.; Mao, L. The relationship between green roofs and urban biodiversity: A systematic review. *Biodivers. Conserv.* **2022**, *31*, 1771–1796. [CrossRef]
13. Czemiel Berndtsson, J. Green roof performance towards management of runoff water quantity and quality: A review. *Ecol. Eng.* **2010**, *36*, 351–360. [CrossRef]
14. Gregoire, B.G.; Clausen, J.C. Effect of a modular extensive green roof on stormwater runoff and water quality. *Ecol. Eng.* **2011**, *37*, 963–969. [CrossRef]
15. Stovin, V.; Vesuviano, G.; Kasmin, H. The hydrological performance of a green roof test bed under UK climatic conditions. *J. Hydrol.* **2012**, *414*, 148–161. [CrossRef]
16. Voyde, E.; Fassman, E.; Simcock, R. Hydrology of an extensive living roof under sub-tropical climate conditions in Auckland, New Zeland. *J. Hydrol.* **2010**, *394*, 384–395. [CrossRef]
17. De-Ville, S.; Menon, M.; Jia, X.; Reed, G.; Stovin, V. The impact of green roof ageing on substrate characteristics and hydrological performance. *J. Hydrol.* **2017**, *547*, 332–344. [CrossRef]
18. Li, Y.; Babcock Jr, R.W. Green roof hydrologic performance and modeling: A review. *Water Sci. Technol.* **2014**, *69*, 4. [CrossRef] [PubMed]
19. Ampim, P.A.Y.; Sloan, J.J.; Cabrera, R.I.; Harp, D.A.; Jaber, F.H. Green Roof Growing Substrates: Types, Ingredients, Composition and Properties. *J. Environ. Hort.* **2010**, *28*, 244–252. [CrossRef]
20. Charpentier, S. Simulation of Water Regime and Sensible Heat Exchange Phenomena in Green Roof Substrates. *Vadose Zone J.* **2015**, *14*, vzj2014-07. [CrossRef]
21. Dauda, I.; Alibaba, H.Z. Green roof benefits, opportunities and challenges. *Int. J. Civ. Struct. Eng. Res.* **2020**, *7*, 106–112.
22. Zhang, S.; Lin, Z.; Zhang, S.; Ge, D. Stormwater retention and detention performance of green roofs with different substrates: Observational data and hydrological simulations. *J. Environ. Manag.* **2021**, *291*, 112682. [CrossRef]
23. Liu, W.; Engel, B.A.; Feng, Q. Modelling the hydrological responses of green roofs under different substrate designs and rainfall characteristics using a simple water balance model. *J. Hydrol.* **2021**, *602*, 126786. [CrossRef]
24. Yio, M.H.N.; Stovin, V.; Werdin, J.; Vesuviano, G. Experimental analysis of green roof substrate detention characteristics. *Water Sci. Technol.* **2013**, *68*, 1477–1486. [CrossRef] [PubMed]
25. Yan, J.; Zhang, S.; Zhang, J.; Zhang, S.; Zhang, C.; Yang, H.; Wang, R.; Wei, L. Stormwater retention performance of green roofs with various configurations in different climatic zones. *J. Environ. Manag.* **2022**, *319*, 115447. [CrossRef] [PubMed]
26. Bortolini, L.; Bettella, F.; Zanin, G. Hydrological Behaviour of Extensive Green Roofs with Native Plants in the Humid Subtropical Climate Context. *Water* **2021**, *13*, 44. [CrossRef]
27. Bettella, F.; D'Agostino, V.; Bortolini, L. Drainage flux simulation of green roofs under wet conditions. *J. Agric. Eng. XLIX* **2018**, *838*, 242–252. [CrossRef]
28. Gan, L.; Garg, A.; Wang, H.; Mei, G.; Liu, J. Influence of biochar amendment on stormwater management in green roofs: Experiment with numerical investigation. *Acta Geophys.* **2021**, *69*, 2417–2426. [CrossRef]
29. Huang, S.; Garg, A.; Mei, G.; Huang, D.; Balaji Chandra, R.; Sadasiv, S.G. Experimental study on the hydrological performance of green roofs in the application of novel biochar. *Hydrol. Process.* **2020**, *34*, 4512–4525. [CrossRef]
30. Quinn, R.; Dussaillant, A. The impact of macropores on heavy metal retention in sustainable drainage systems. *Hydrol. Res.* **2018**, *49*, 517–527. [CrossRef]
31. Liu, R.; Fassman-Beck, E. Hydrologic response of engineered media in living roofs and bioretention to large rainfalls: Experiments and modeling. *Hydrol. Process.* **2017**, *31*, 556–572. [CrossRef]
32. Hilten, R.N.; Lawrence, T.M.; Tollner, E.W. Modeling stormwater runoff from green roofs with HYDRUS-1D. *J. Hydrol.* **2008**, *358*, 288–293. [CrossRef]

33. Brunetti, G.; Šimůnek, J.; Piro, P. A Comprehensive Analysis of the Variably Saturated Hydraulic Behavior of a Green Roof in a Mediterranean Climate. *Vadose Zone J.* **2016**, *15*, vzj2016.2004.0032. [CrossRef]
34. Li, Y.; Babcock Jr, R.W. Modeling Hydrologic Performance of a Green Roof System with HYDRUS-2D. *J. Environ. Eng.* **2015**, *141*, 04015036. [CrossRef]
35. Soulis, K.X.; Valiantzas, J.D.; Ntoulas, N.; Kargas, G.; Nektarios, P.A. Simulation of green roof runoff under different substrate depths and vegetation covers by coupling a simple conceptual and a physically based hydrological model. *J. Environ. Manag.* **2017**, *200*, 434e445. [CrossRef] [PubMed]
36. Kasmin, H.; Stovin, V.R.; Hathway, E.A. Towards a generic rainfall-runoff model for green roofs. *Water Sci. Technol.* **2010**, *62*, 898–905. [CrossRef]
37. Locatelli, L.; Mark, O.; Mikkelsen, P.S.; Arnbjerg-Nielsen, K.; Bergen Jensen, M.; Binning, P.J. Modelling of green roof hydrological performance for urban drainage applications. *J. Hydrol.* **2014**, *519*, 3237–3248. [CrossRef]
38. Stovin, V.; Poë, S.; De-Ville, S.; Berretta, C. The influence of substrate and vegetation configuration on green roof hydrological performance. *Ecol. Eng.* **2015**, *85*, 159–172. [CrossRef]
39. De-Ville, S.; Menon, M.; Stovin, V. Temporal variations in the potential hydrological performance of extensive green roof systems. *J. Hydrol.* **2018**, *558*, 564–578. [CrossRef]
40. Lönnqvist, J.; Broekhuizen, I.; Viklander, M.; Blecken, G. Green roof runoff reduction of 84 rain events: Comparing Sedum, life strategy-based vegetation, unvegetated and conventional roofs. *J. Hydrol.* **2025**, *646*, 132325. [CrossRef]
41. Peng, Z.; Smith, C.; Stovin, V. Internal fluctuations in green roof substrate moisture content during storm events: Monitored data and model simulations. *J. Hydrol.* **2019**, *573*, 872–884. [CrossRef]
42. Skala, V.; Dohnal, M.; Votrubová, J.; Jelínková, V. The use of simple hydrological models to assess outflow of two green roofs systems. *Soil Water Res.* **2019**, *14*, 94–103. [CrossRef]
43. Bondì, C.; Alagna, V.; Iovino, M. Hydrological response of a volcanic medium as a potential substrate for green roofs. In Proceedings of the IEEE International Workshop on Metrology for Agriculture and Forestry (MetroAgriFor), Pisa, Italy, 6–8 November 2023.
44. Autovino, D.; Alagna, V.; Bondì, C.; Iovino, M. Hydraulic Characterization of Green Roof Substrates by Evaporation Experiments. *Appl. Sci.* **2024**, *14*, 1617. [CrossRef]
45. Wind, G.P. Capillary Conductivity Data Estimated by a Simple Method. In *Water in the Unsaturated Zone, Proceedings of the Wageningen Symposium, Wageningen, The Netherlands, 19–23 June 1966*; Institute for Land and Water Management Research: Wageningen, The Netherlands, 1969; Volume 1, p. 1.
46. Dane, J.H.; Hopmans, J.W. Pressure Plate Extractor. In *Methods of Soil Analysis, Part 4, Physical Methods*; Dane, J.H., Topp, G.C., Eds.; Soil Science Society of America, Inc.: Madison, WI, USA, 2002; pp. 680–683.
47. van Genuchten, M.T. A Closed-Form Equation for Predicting the Hydraulic Conductivity of Unsaturated Soils. *Soil Sci. Soc. Am. J.* **1980**, *44*, 892–898. [CrossRef]
48. De-Ville, S.; Stovin, V. Application of a Conceptual Hydrological Model to Identify the Impacts of Green Roof Substrate Ageing on Detention Performance. In Proceedings of the University of Sheffield Engineering Symposium Conference Proceedings Volume 1, USES 2014, Sheffield, UK, 24 June 2014; The University of Sheffield: Sheffield, UK, 2014.
49. Lilliefors, H.W. On the Kolmogorov-Smirnov test for normality with mean and variance unknown. *J. Am. Stat. Assoc.* **1967**, *62*, 339–402. [CrossRef]
50. Nash, J.E.; Sutcliffe, J.V. River flow forecasting through conceptual models part I—A discussion of principles. *J. Hydrol.* **1970**, *10*, 282–290. [CrossRef]
51. Bondì, C.; Concialdi, P.; Iovino, M.; Bagarello, V. Assessing short- and long-term modifications of steady-state water infiltration rate in an extensive Mediterranean green roof. *Heliyon* **2023**, *9*, e16829. [CrossRef]
52. Liu, W.; Feng, Q.; Chen, W.; Wei, W. Assessing the runoff retention of extensive green roofs using runoff coefficients and curve numbers and the impacts of substrate moisture. *Hydrol. Res.* **2020**, *51*, 635–647. [CrossRef]
53. Villarreal, E.L.; Bengtsson, L. Response of a Sedum green-roof to individual rain events. *Ecol. Eng.* **2005**, *25*, 1–7. [CrossRef]
54. Breulmann, M.; Merbach, A.; Bernhard, K.; Moeller, L. Enhancing Urban Resilience: Stormwater Retention and Evapotranspiration Performance of Green Roofs Under Extreme Rainfall Events. *Land* **2025**, *14*, 977. [CrossRef]
55. Cui, E.; Fu, X.; Yang, X.; Zhang, Q.; Duan, D.; Hopton, M. How vertical drainage positions of extensive green roofs affect the runoff control performance. *J. Hydrol.* **2024**, *642*, 131855. [CrossRef]
56. Stovin, V. The potential of green roofs to manage Urban Stormwater. *Water Environ. J.* **2010**, *24*, 192–199. [CrossRef]
57. Volder, A.; Dvorak, B. Event size, substrate water content and vegetation affect storm water retention efficiency of an un-irrigated extensive green roof system in Central Texas. *Sustain. Cities Soc.* **2014**, *10*, 59–64. [CrossRef]
58. Zheng, X.; Zou, Y.; Lounsbury, A.W.; Wang, C.; Wang, R. Green roofs for stormwater runoff retention: A global quantitative synthesis of the performance. *Resour. Conserv. Recycl.* **2021**, *170*, 105577. [CrossRef]

59. Wang, J.P.; Liu, T.H.; Wang, S.H.; Luan, J.Y.; Dadda, A. Investigation of porosity variation on water retention behaviour of unsaturated granular media by using pore scale Micro-CT and lattice Boltzmann method. *J. Hydrol.* **2023**, *626*, 130161. [CrossRef]
60. Gerke, H.H.; van Genuchten, M.T. A dual-porosity model for simulating the preferential movement of water and solutes in structured porous media. *Water Resour. Res.* **1993**, *29*, 305–319. [CrossRef]
61. Russell, A.R. Water retention characteristics of soils with double porosity. *Eur. J. Soil Sci.* **2010**, *61*, 412–424. [CrossRef]
62. Pęczkowski, G.; Szawernoga, K.; Kowalczyk, T.; Orzepowski, W.; Pokładek, R. Runoff and Water Quality in the Aspect of Environmental Impact Assessment of Experimental Area of Green Roofs in Lower Silesia. *Sustainability* **2020**, *12*, 4793. [CrossRef]
63. Wu, L.; Peng, M.; Qiao, S.; Ma, X. Effects of rainfall intensity and slope gradient on runoff and sediment yield characteristics of bare loess soil. *Environ. Sci. Pollut. Res.* **2018**, *25*, 3480–3487. [CrossRef]
64. Ferrans, P.; Rey, C.V.; Pérez, G.; Rodrìguez, J.P.; Dìaz-Granados, M. Effect of Green Roof Configuration and Hydrological Variables on Runoff Water Quantity and Quality. *Water* **2018**, *10*, 960. [CrossRef]
65. Stovin, V.; Vesuviano, G.; De-Ville, S. Defining green roof detention performance. *Urban Water J.* **2017**, *14*, 574–588. [CrossRef]